THE JOURNAL OF PHYSICAL CHEMISTRY A
A JOURNAL OF THE AMERICAN CHEMICAL SOCIETY

pubs.acs.org/JPCA
Article

High Resolution Leak-Out Spectroscopy of the ν_2 Symmetric CH_3 Stretching Mode of Protonated Acetonitrile, CH_3CNH^+

Published as part of The Journal of Physical Chemistry A special issue "Mark A. Johnson Festschrift".

Thomas Salomon, Weslley G. D. P. Silva, Sven Thorwirth, Oskar Asvany, and Stephan Schlemmer*

Cite This: J. Phys. Chem. A 2026, 130, 88−95

Read Online

ACCESS | Metrics & More | Article Recommendations | Supporting Information

ABSTRACT: The symmetric CH_3 stretching mode ν_2 of protonated acetonitrile (CH_3CNH^+), located around 3.4 μm, has been measured at high resolution in a cryogenic 22-pole ion trap apparatus via leak-out spectroscopy. In addition to this fundamental vibrational mode, several close-lying combination bands interfering through Fermi-resonances were detected in its proximity. Two of those have been assigned as the $\nu_5 + 2\nu_8$ and $\nu_5 + \nu_7 + \nu_9$ combination bands, and three more likely arising from the four-quanta combination mode, $\nu_7 + 2\nu_9 + \nu_{10}$. The formation of ground-state combination differences permits the spectroscopic assignment of 227 out of the 261 detected lines. A thorough treatment of the Fermi resonance system yields spectroscopic constants for three of the bands and approximate spectroscopic constants for all remaining ones.

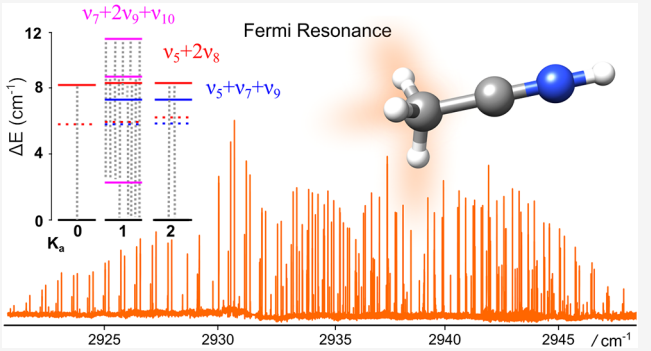

INTRODUCTION

Methyl cyanide, CH_3CN, was detected as early as 1971 in the interstellar medium (ISM)[1] and since then has been found to be very abundant in diverse astrophysical environments (see, e.g., Giani et al.[2] and references therein). Because of its high proton affinity of 788(8) kJ/mol,[3] CH_3CNH^+ is considered a plausible target for astronomical searches but remains undetected thus far.[4]

The first laboratory spectroscopic investigation of CH_3CNH^+ by Amano[5] targeted the fundamental ν_1 N−H stretching mode at about 3500 cm^{-1}. Some years later, a pure rotational spectrum of CH_3CNH^+ could also be recorded[6,7] yielding accurate molecular parameters of the ground vibrational state. Most recently, a low-resolution infrared overview spectrum of CH_3CNH^+, obtained by predissociating the Ne-tagged species and assigned with the help of high-level *ab initio* calculations,[8] revealed the positions of all vibrational bands of CH_3CNH^+ in the range from 380 to 3600 cm^{-1}.

This work reports on the first rotationally resolved observation of the ν_2 symmetric CH_3 stretching band of CH_3CNH^+, employing leak-out spectroscopy (LOS).[9] As it turns out, this band is accompanied by several combination bands of the same symmetry, establishing a complex system exhibiting Fermi interactions. Analysis of these interactions and determination of respective effective molecular parameters is the central aim of this work.

EXPERIMENTAL METHODS

The experiments of this study were carried out in the cryogenic 22-pole ion trapping instrument COLTRAP.[10] In brief, CH_3CNH^+ ions were generated in a storage ion source by electron impact ionization of CH_3CN vapor. Every second, a pulse of several ten-thousand ions was extracted from the source, selected in a quadrupole mass spectrometer for a mass to charge ratio m/z = 42, and then injected into the 22-pole trap.[11] The trap was held at a nominal temperature of T = 4 K and constantly filled with He buffer gas (~10^{13} cm^{-3}). For performing vibrational spectroscopy of the trapped ions, the novel leak-out action spectroscopy method (LOS[9]) has been applied. This technique has proven to be quite universal and effective, with numerous recent applications to astrophysically relevant cations.[9,12−21] In brief, LOS exploits the fact that the vibrational energy of a laser-excited ion can be converted into kinetic energy in a collision with a suitable neutral molecule or atom. In this work neon has been used as the collision partner, which was additionally pulsed into the ion trap as a 3:1 He/Ne gas mixture. After the energy exchange, the accelerated

Received: September 10, 2025
Revised: October 26, 2025
Accepted: October 27, 2025
Published: December 23, 2025

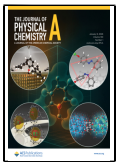

CH_3CNH^+ ions may then escape the ion trap and can be counted in a Daly type ion detector. By repeating these cycles at 1 Hz, and counting the "leaked-out" CH_3CNH^+ ions as a function of the laser wavenumber, a spectrum is obtained. The infrared excitation was supplied by a continuous wave optical parametric oscillator (cw-OPO, Toptica, model TOPO) operating in the 2.5−3.5 μm spectral region. The bandwidth of the OPO radiation is typically very narrow (<MHz) and thus much narrower than the Doppler widths of the recorded transitions. The power of the OPO was on the order of a few hundred mW. The frequency of the IR radiation was measured continuously by a wavemeter/spectrum analyzer (Bristol Instruments, model 771A-MIR), which has an absolute accuracy of 0.2 ppm, i.e., about 0.001 cm^{-1}.

QUANTUM CHEMICAL CALCULATIONS

Results of high-level CCSD(T) calculations of CH_3CNH^+ using various basis sets have been reported elsewhere recently[8] summarizing structural parameters, rotation-vibration interaction parameters as well as vibrational wavenumbers. In the present study, not least for practical purposes, spectroscopic analysis of the CH_3CNH^+ spectra has been based on calculations performed at the CCSD(T)/ANO1 level of theory in the frozen core (fc) approximation. This level has been shown earlier to provide force fields of high quality[22] and will also be applicable to molecules more complex than CH_3CNH^+ studied here. Corresponding harmonic and anharmonic vibrational wavenumbers of CH_3CNH^+ have already been tabulated in ref 8, but rotation-vibration interaction parameters α_i and l-type doubling constants q_i are collected here in Table 1. All calculations were performed using the CFOUR program[23,24] using strategies outlined in detail elsewhere.[25]

As the A_0 rotational constant of CH_3CNH^+ is not determinable from the measurements performed here nor in earlier studies, a best estimate value has been calculated using isostructural and isoelectronic CH_3CCH as calibrator. For the latter species the calculated constant $A_{0,calc}$ is obtained as 159,121.346 MHz using the CCSD(T)/cc-pwCVQZ equilibrium rotational constant (derived with all electrons being considered in the correlation treatment) and the CCSD(T)/ANO1 zero-point vibrational correction. Comparing this value against the experimental $A_{0,exp}$ = 159140.33 MHz from ref 26 yields a ratio of $A_{0,exp}/A_{0,calc}$ = 1.000119. Applying this as a calibration factor to $A_{0,calc}$ of CH_3CNH^+ provides a best estimate A_0 value of 154,952.4 MHz. This value has been kept fixed in the spectroscopic analysis presented here in the following. It is worthwhile mentioning that similar calculations of isoelectronic methyl cyanide, CH_3CN, employing analogous levels of theory and the most recent $A_{0,exp}$ = 158,098.91 MHz value from experiment[27] results in a ratio $A_{0,exp}/A_{0,calc}$ = 1.000032, even closer to unity. This suggests that the strategy used here is adequate to derive very good estimates of ground state rotational constants of this family of symmetric top species. For the sake of completeness, the calculated and scaled B_0 rotational constant of CH_3CNH^+ is 8587.895 MHz, agreeing to within 0.03% with the experimental value of 8590.559 MHz, as obtained by Amano et al.[6] and Gottlieb et al.[7]

Table 1. Calculated (CCSD(T)/ANO1) Rotation-Vibration Interaction Terms, α_i^A and α_i^B, as well as l-type Doubling (q_i) Constants of the Fundamental Vibrational Modes ν_i of CH_3CNH^+

mode	sym.	harm. (cm^{-1})	anharm. (cm^{-1})	α_i^A (MHz)	α_i^B (MHz)	q_i (MHz)
ν_{10}-CCN bending	E	381	384	92.4	−20.1	14.72
ν_9-CNH bending	E	580	579	29.5	−8.0	8.92
ν_8-CH_3 wagging	E	1048	1023	−876.7	−0.1	3.64
ν_7-CH_3 scissoring	E	1442	1428	890.5	−37.2	59.6
ν_6-CH_3 asym. stretching	E	3149	2999	1214.3	1.0	0.62
ν_5-CC stretching	A_1	897	887	259.5	51.0	...
ν_4-CH_3 umbrella	A_1	1393	1358	−929.1	67.1	...
ν_3-CN stretching	A_1	2345	2300	105.4	44.3	...
ν_2-CH_3 sym. stretching	A_1	3049	2927	1645.9	2.3	...
ν_1-NH stretching	A_1	3699	3534	−27.0	21.1	...

RESULTS

Spectroscopic searches for the ν_2 mode of CH_3CNH^+ (A_1-symmetry) started around its predicted band center at 2927 cm^{-1} (Table 1), which is also in agreement with results of recent Ne-tagging measurements.[8] A sequence of lines has been readily detected which resembles that of parallel transitions belonging to a prolate symmetric top. The recorded high-resolution spectrum is shown in the upper trace of Figure 1. The lower traces show the simulated spectrum and respective subbands as discussed individually below.

Due to the low trap temperature and a large A_0 rotational constant, only transitions of ν_2 originating from K = 0, 1, 2 should be detected. While the spectrum at its low frequency end exhibits a typical set of close lying lines of a P-branch with the respective K subbands, the spectrum becomes much busier above 2930 cm^{-1}. This finding already shows that the spectrum is comprised of a set of close lying vibrational bands. The richness and the complexity of the high-resolution spectrum are illustrated in more detail by the inset in Figure 1 which already shows the good agreement of our simulation and the experimental spectrum as will be discussed in detail in this work.

Despite the complexity of the subbands with K = 1 and K = 2, Q-branches of the ν_2 band could be identified at about 2929.32 and 2929.25 cm^{-1}, respectively, and the band center of the K = 0 subband (without Q-branch) was identified at 2929.46 cm^{-1}. This assignment is illustrated by the simulated spectrum for the K = 0 subband as a blue trace in Figure 1.

An analysis of the observed line widths (FWHM ≈ 60 MHz) yields a kinetic temperature of about T_{kin} ≈ 20 K, and a comparison of the line intensity distribution for the dominant ν_2 band with a simulation obtained with PGOPHER[28] (Figure 1), gives an estimate of the rotational temperature of about T_{rot} = 12 K. A list of all observed lines and their respective assignment is given in the Supporting Information. The agreement of the measured leak-out signal and the simulated intensities as is visible in Figure 1 helped the further assignment and the analysis of the more busy part of the spectrum.

https://doi.org/10.1021/acs.jpca.5c06360
J. Phys. Chem. A 2026, 130, 88−95

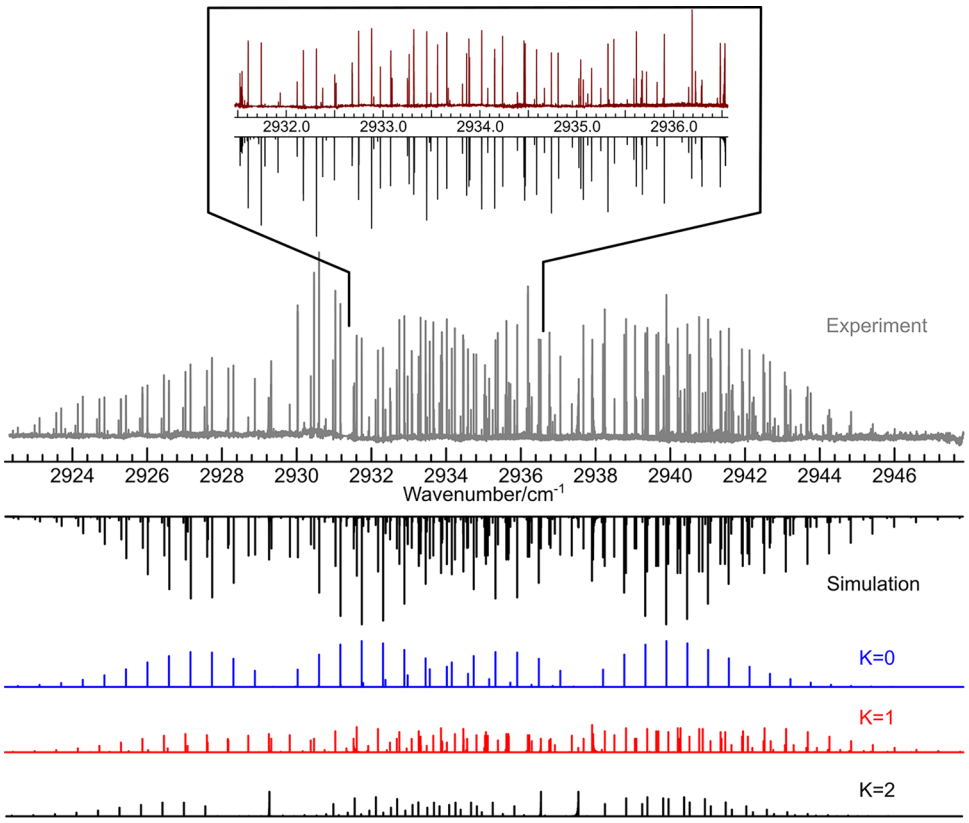

Figure 1. LOS spectrum of the ν_2 symmetric CH_3 stretching resonance system of CH_3CNH^+. The upper part shows the experimental spectrum, the lower part is a stick spectrum simulated at a temperature of 12 K using the fitted parameters from Table 3. The (tentative) assignment to individual vibrational bands is discussed in the text.

SPECTROSCOPIC ANALYSIS

Due to the perturbed character of the ν_2 resonance system, the further analysis has been started with the identification of additional subbands, i.e., those with $K = 0, 1, 2$. While such an identification turned out to be relatively straightforward in the lower wavenumber part of the spectrum, the subbands at higher wavenumbers are challenging to assign because of an interfering forest of unidentified lines. Nonetheless, besides the subbands of the ν_2 band mentioned above, an additional Q-branch at 2937.54 cm^{-1} and a skewed Q-branch at 2937.91 cm^{-1} have been readily identified. The structure of those subbands with $K = 2$ and $K = 1$, respectively, follow the typical patterns of missing lines for $J < K$.

A ground state combination difference (GSCD) fit of all these components reveals that all of them originate from the same ground vibrational state. The ground state rotational constant B_0 obtained through this analysis agrees to within experimental uncertainty with the value from the pure rotational data reported by Amano et al.[6] and Gottlieb et al.[7] (Table 2), unequivocally confirming CH_3CNH^+ as being the carrier of the spectroscopic signature. Therefore, in the rest of this work, those highly accurate ground state rotational constants are used for our further analysis. Moreover, since all observed lines arise from the same vibrational ground state term pattern of a prolate symmetric top, the band centers found in the spectrum are ordered by the vibrational energies of the respective bands. This is why the bands found were numbered in this order in Table 3 by giving them Roman numbers (I–VI). By the same argument the $K = 0, 1, 2$ subbands have been ordered and assigned to these respective bands.

Table 2. Spectroscopic Parameters Obtained via an Effective Hamiltonian Analysis of Ground State Combination Differences (GSCD)[a]

	GSCD	Amano et al.[6]	Gottlieb et al.[7]
B_0 (MHz)	8590.61(16)	8590.5589(10)	8590.55675
D_J (kHz)	5.2(8)	3.14078(77)	3.125
D_{JK} (kHz)	188(40)	163.30(33)	156.75

[a]The obtained values are compared to those derived from pure rotational measurements reported by Amano et al.[6] and Gottlieb et al.[7] Experimental uncertainties are given in parentheses.

Based on these findings, an assignment of the yet unidentified lines was performed by forming blind combination differences, and searching for the known GSCDs derived from the accurate mm-wave data,[6] a procedure proven before to work very well.[16,29] Following this procedure, a total of two subbands with $K = 0$, six with $K = 1$, and three with $K = 2$ were identified in the experimental spectrum, see Table 3. Overall, 227 out of 261 observed transitions of the ν_2 system could be assigned (for $K = 0, 1, 2$) with confidence. Notably, in the spectrum shown in Figure 1, only 34 lines remain unassigned.

With the assignments of six bands, and with the ground state parameters fixed to the high-resolution mm-wave and ab initio values provided in the literature[6,30] as listed in Table 2, it has been attempted to fit the data using a prolate symmetric top Hamiltonian as implemented in PGOPHER.[28] Rigid rotor fits of individual K-stacks are found to work well. The results of these fits are those displayed in Table 3. For each K subband

https://doi.org/10.1021/acs.jpca.5c06360
J. Phys. Chem. A 2026, 130, 88−95

Table 3. Spectroscopic Parameters[a] for the Six Measured Bands of the ν_2 Resonance System of CH_3CNH^+ and Their Respective K Subbands are Given Ordered by the Band Center Frequency[c]

		I	II	III	IV	V	VI
$K_a = 0$	ν (cm^{-1})	2929.4557(6)	...	...	2937.6308(6)	...	...
	B	8581.7(2)	...	...	8550.7(2)	...	...
	α^{B}[b]	8.9(2)	...	...	39.9(2)	...	...
$K_a = 1$	ν (cm^{-1})	2929.3202(6)	2931.5212(7)	2936.5356(6)	2937.9068(6)	2937.9342(6)	2940.2211(6)
	B	8582.8(2)	8669.3(4)	8571.3(4)	8591.7(3)	8661.5(7)	8605.0(3)
	α^{B}[b]	7.8(2)	−78.7(4)	19.6(4)	−1.1(3)	−70.9(7)	−14.4(3)
$K_a = 2$	ν(cm^{-1})	2929.2564(6)	...	2936.5440(8)	2937.5508(6)	...	...
	B	8581.6(3)	...	8578.5(3)	8554.5(4)	...	...
	α^{B}[b]	9.0(3)	...	12.1(3)	36.1(4)	...	...

[a]The A rotational constant is fixed to its ground state value. [b]Values for α^B are derived from the fitted B rotational constants for each band and the highly accurate ground state values from literature, Amano et al.[6] and Gottlieb et al.[7] [c]All values in MHz unless otherwise noted. Experimental uncertainties are given in parentheses.

an individual band origin and a rotational constant has been determined for the series of lines in the respective subband. From the latter value and the highly accurate ground state rotational constants the rotation-vibration interaction constant α^B is determined and also listed in Table 3. Comparison to the theoretical values of α^B shall help later-on in the identification of the vibrational bands involved in this ν_2 symmetric CH_3 stretching resonance system of CH_3CNH^+.

With the identification of the six bands it is tempting to connect the individual K-stacks belonging to one band. However, this approach failed because a large variety of unphysically large centrifugal correction terms (e.g., D_K) were required to fit the measured spectrum. In addition, the $K = 0$ subbands are missing for four of the six bands. Although the subband origins are sorted coarsely by the bands, each system of subbands appears to be shifted for the individual K-stacks, while leaving their rotational progressions largely unaffected. These findings are clear indications of a system of interacting vibrational bands, an observation which has been made previously for similar molecules.

Fermi resonances are known to occur for similar vibrational modes of other methyl compounds, such as the isoelectronic and isostructured methyl acetylene CH_3CCH,[31] for which the A_1-symmetry components of the doubly excited CH_3 deformation vibrations $2\nu_4$ (CH_3 umbrella vibration) and $2\nu_7$ (CH_3 scissoring vibration) are relatively close in energy to the ν_2 symmetric CH_3 stretching mode, allowing for sizable intensity borrowing. Even for the ν_1 NH stretching band of CH_3CNH^+, a K-dependent perturbation has been observed in the pioneering work of Amano.[5] In that case, $K = 2$ lines were perturbed most severely, and only a few lines could be identified. Amano suggested that the perturbing state affecting the $K = 1$ series involves the excitation of several quanta of low-lying vibrational modes, and that the interaction is also likely to be of Fermi-type.

Similarly, for the present case of the ν_2 vibrational mode, the number of interacting states seems to vary depending on the K quantum number, as indicated by the different number of identified K-stacks (see Table 3). Hence, a global fit ignoring the interaction of bands would have a highly effective character with little physical meaning of the obtained spectroscopic parameters, which is why connecting the K-stacks failed in the first place. Still, the association of the subbands with their band seems clear due to the proximity of the respective band origins, see Table 3, and it is the task of a deperturbation treatment to find the one band origin for all subbands and to obtain a common fit of the rotational structure of each band.

The mixing in this multilevel Fermi resonance system appears to be strongest for the $K = 1$ configuration, as a larger number of subbands gain sufficient intensity through intensity borrowing. The symmetry of the resonance partners has to be equivalent to that of the ν_2 fundamental (A_1) to be in Fermi-resonance and gain intensity from it. Furthermore, these interacting vibrational states have to be reasonably close in energy compared to the ν_2 vibrational fundamental. For that reason, all combination bands calculated to be within ±50 cm^{-1}, and having at least one A_1 symmetry component, were identified and considered in the following analysis and discussion. Four such combination bands are displayed in the left panel of Figure 2 based on the calculated term energies together with their vibrational modes. Based on the symmetry of the participating vibrations the symmetries of the resulting vibrational species are calculated and also given in Figure 2. As a result, all combination bands contain at least one A_1

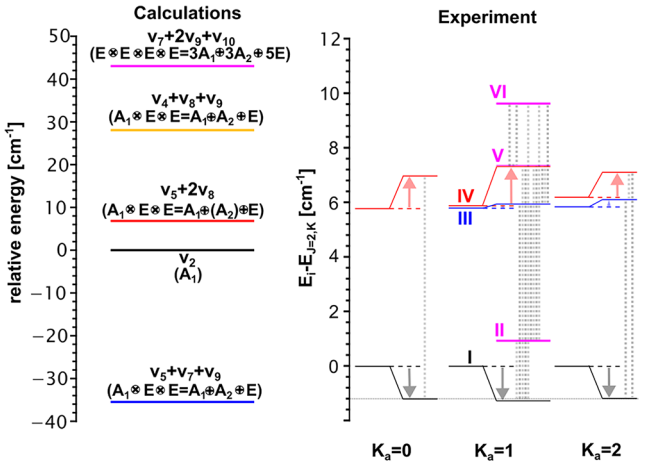

Figure 2. (Left) Energy term scheme of the Fermi-resonance system calculated at the CCSD(T)/ANO1 level of theory. The symmetries of the individual components of each combination band are listed in brackets, while only the components of A_1 vibrational symmetry are plotted. The energy term values of the $\nu_7 + 2\nu_9 + \nu_{10}$ mode are estimated by combining anharmonic frequencies of the involved vibrational fundamentals. (Right) Perturbed (solid horizontal lines) and unperturbed (dashed horizontal lines) term energies of the ν_2 resonance system. The gray vertical dashed lines indicate the Fermi interaction terms affecting the individual K-stacks.

https://doi.org/10.1021/acs.jpca.5c06360
J. Phys. Chem. A 2026, 130, 88−95

symmetry component which can be in resonance with the ν_2 vibrational fundamental (A_1). In total, three possible resonating combination bands are found in proximity to the ν_2 symmetric CH_3 stretching vibration, involving up to three vibrational quanta. These combination bands are $\nu_5 + 2\nu_8$, $\nu_5 + \nu_7 + \nu_9$ as well as $\nu_4 + \nu_8 + \nu_9$, and involve the low lying CH_3 wagging (ν_8), scissoring (ν_7) and umbrella (ν_4) vibrations which are known to notoriously cause resonances with the CH_3-stretching vibrations (c.f. ref 31). Figure 2 also displays the four quanta combination band $\nu_7 + 2\nu_9 + \nu_{10}$ due to its proximity to ν_2.

In the simplest case of a Fermi resonance, two vibrational modes of the same vibrational symmetry and the same rotational state (J, K) are interacting. Our spectrum exhibits such a system of two interacting $K = 0$ subbands for the bands I and IV listed in Table 3. The result of the Fermi resonance pushes the lower energy (E_I) level down and the higher one (E_{IV}) up.

This apparent repulsion between two such interacting vibrational states depends on three major factors: the magnitude of the anharmonic coupling term $H_{I,IV}$, the degree to which the wave functions of the two interacting states overlap with each other, as well as the separation $\Delta E_{I,IV}$ between the unperturbed vibrational levels E_I, E_{IV}. The effect of the additional term $H_{I,IV}$ arising in the stationary Schrödinger equation of a coupled system is usually summarized as the coupling strength $W_{I,IV} = \langle \psi_I | H_{I,IV} | \psi_{IV} \rangle$, which also involves the influence of the overlap between the vibrational wave functions. For the simplest case of the two-level Fermi resonance system, one finds that the energies of the perturbed states $E'_{I,IV}$ are given by

$$E'_{I,IV} = \frac{E_I(J,K) + E_{IV}(J,K)}{2} \pm \frac{\sqrt{\Delta E_{I,IV}(J,K)^2 + 4W_{I,IV}(J,K)^2}}{2} \quad (1)$$

The repulsion is largest and equals to $W_{I,IV}(J,K)$ on resonance ($\Delta E_{I,IV}(J,K) = 0$) and decreases rapidly $\sim W_{I,IV}(J,K)^2/\Delta E_{I,IV}(J,K)$ as the energy difference of the unperturbed states increases, which is why only close lying vibrational states are considered.

The effect of this repulsion can be seen for the two interacting $K = 0$ subbands in the right panel of Figure 2. There the vibrational energies for the ($J = 2$, $K = 0$) rotational states of the interacting ν_I and ν_{IV} levels are shown as solid lines while the unperturbed levels correspond to the dashed lines. The assignment $\nu_I = \nu_2$ and $\nu_{IV} = \nu_5 + 2\nu_8$ is suggested already by the proximity of the calculated vibrational frequencies as seen in the left panel of Figure 2, notice the color coding of the calculated bands (left panel) and measured band positions (right panel). However, additional arguments for the band assignments will be given below. The repulsion of the two levels is depicted as the two arrows indicating the shifts down and up of the unperturbed levels. In fact, the values displayed in Figure 2 are the result of a deperturbation treatment where $W^2_{I,IV}/\Delta E_{I,IV}(J,K)$ is determined from a simultaneous fit of both subbands as employed in the PGOPHER[28] program. The resulting band positions and Fermi interaction term $W_{I,IV}$ are listed in Table 4 together with other parameters which will be discussed in the following where also the $K = 1$, 2 subbands are considered.

The separation $\Delta E_{I,IV}(J,K)$ varies with J and K due to the different rotation-vibration interaction constants α^A_i, α^B_i, for the different vibrational modes. Since the α^A_i constants are much larger than the α^B_i, as seen in Table 1, $\Delta E_{I,IV}(J,K)$ is dominated by its variation with K, which is one reason why only two bands interact for $K = 0$ but three for $K = 2$ and even six for $K = 1$ as identified in Table 3.

The deperturbation approach makes use of this fact, and a sequential deperturbation fit using PGOPHER[28] has been performed starting the analysis with the two-level resonance system $K = 0$, increasing the complexity of the PGOPHER model to simulate the $K = 2$ subband, before trying to deperturb the most complicated six-level interaction system seen for $K = 1$. As a result, Fermi interaction terms $W_{A,B}(K)$ for each pairwise interacting vibrational K subbands of vibrational states A and B will be derived.

For $K = 0$, only a single interaction term, $W_{I,IV}(K = 0) = W_{I,IV}$ in Table 4, indicated by the dashed vertical line in the right-hand panel of Figure 2, has to be implemented, leading to a stringent convergence of the least-squares fit of PGOPHER as discussed above. The rotation-vibration interaction constants α^B_i derived from the deperturbation of the two $K = 0$ subbands, as given in Table 4, are in quantitative agreement with the rotation-vibration coupling constants calculated for the ν_2 vibrational fundamental ($\alpha^B_{\nu_2} = 2.3$ MHz) and the $\nu_5 + 2\nu_8$ ($\alpha^B_{\nu_5} + 2\alpha_{\nu_8} = 50.8$ MHz) combination band determined in the quantum chemical calculations listed in Table 1. This gives us confidence to perform a proper deperturbation and a proper assignment of $\nu_I = \nu_2$ and $\nu_{IV} = \nu_5 + 2\nu_8$.

For the unperturbed levels as indicated by the dashed color-coded horizontal lines in the right panel of Figure 2, an energy difference of about 5.8 cm^{-1} has been determined. This value is in very good agreement with our calculated difference of 6.7 cm^{-1} as seen in the left panel of Figure 2. This gives us further confidence of the right assignment of the interacting vibrational bands as discussed above.

Table 4. Molecular Parameters Derived from Deperturbing the $K = 0$, 2 Components in PGOPHER[28a]

band	parameter	$K_a = 0$, 2
I (ν_2)	ν/cm^{-1}	2930.64295(7)
	A/MHz[b]	153288.035
	α^B/MHz[c]	2.2(2)/2.3[b]
	D_J/kHz	4(1)
IV ($\nu_5 + 2\nu_8$)	ν/cm^{-1}	2936.44317(15)
	A/MHz[b]	156427.835
	α^B/MHz[c]	46.4(2)/50.8[b]
	D_J/kHz	3(1)
III ($\nu_5 + \nu_7 + \nu_9$)	ν/cm^{-1}	2936.0995(17)
	A/MHz[b]	153754.435
	α^B/MHz[c]	5.9(23)/5.8[b]
	D_J/kHz	86(17)
Fermi interaction terms	$W_{I,IV}$/cm^{-1}	2.88057(7)
	$W_{K^2,I,IV}$/cm^{-1}	−0.262(6)
	$W_{I,III}$/cm^{-1}	2.09(2)
	$W_{III,IV}$/cm^{-1}	−1.077(5)

[a]The assignment of the individual bands to their respective vibrational modes is based on a best match between the derived rotation-vibration interaction constants and the respective theoretical values. [b]Value derived from our CCSD(T)/ANO1 quantum chemical calculations (Table 1). [c]Values for α^B are derived from the fitted B rotational constants for each band and the highly accurate ground state values from literature, Amano et al.[6] and Gottlieb et al.[7]

https://doi.org/10.1021/acs.jpca.5c06360
J. Phys. Chem. A 2026, 130, 88−95

For the $K = 2$ subbands, in total, three terms for the Fermi interaction of three interacting vibrational bands had to be considered. Fortunately, the band centers of bands I and IV, as well as their rotation-vibration interaction constants, α_i^B, are already known from the $K = 0$ subband, which is why these values are kept fixed for the fit of the $K = 2$ subband. A simultaneous fit of the A rotational constants as well as Fermi interaction terms did not succeed, as both parameters are highly correlated. Hence, the predicted A rotational constants derived from the quantum chemical calculations listed in Table 1 have been fixed for subbands I and IV. In contrast, that of the third yet unknown, combination band III is initially fixed to the value of the ν_2 fundamental while fitting its band center. That initial deperturbation fit indicated that the third interacting combination band possesses a rotation-vibration interaction constant $\alpha_{III}^B = 5.9(11)$ MHz, which, although having a rather large uncertainty, matches quite well the B-type rotation-vibration interaction constant predicted for the $\nu_5 + \nu_7 + \nu_9$ combination band ($\alpha_{\nu_5}^B + \alpha_{\nu_7}^B + \alpha_{\nu_9}^B = 5.8$ MHz, values from Table 1). With this suggestive agreement, the $K = 2$ subband is fitted while fixing the A rotational constants to their individual estimates derived from our calculations, yielding the molecular parameters listed in Table 4. Releasing the centrifugal distortion constants in this fit has proved necessary due to a clear $J^2(J + 1)^2$ trend in the fitting residuals when fixed to the ground state value. As this is not observed for the $K = 0$ subband, it is speculated that a weak Coriolis coupling term to an unidentified band, which exhibits a crossing at higher rotational states, might also affect the $K = 2$ subband.

The result of this deperturbation treatment is seen in the right panel of Figure 2 for the $K = 2$ energy levels. Again, the solid lines mark the shifted energy terms as determined from the experiment while the dashed lines mark the energy terms of the corresponding unperturbed states. As for $K = 0$ the energy axis (for all K stacks) is calibrated to the term energy of the unperturbed ν_2 state for $J = 2$ in order to visually compare the Fermi resonance terms. Since the A rotational constants are not known from experiment the calculated values as listed in Table 4 have been adopted and used in the subband fits discussed so far for this energy reference. Inspection of the right panel of Figure 2 for $K = 2$ reveals that the ν_2 state is pushed down by about the same amount as for the $K = 0$ case where only two vibrations interact. The $\nu_5 + 2\nu_8$ state is pushed up less and the final $\nu_5 + \nu_7 + \nu_9$ state is shifted up much less than the two other levels.

Applying the same approach used to disentangle the Fermi-resonance system in the $K = 0$ and $K = 2$ subbands on the $K = 1$ subband, unfortunately, did not result in converging fits. This finding is attributed to the complexity of the Fermi resonance system, as 15 independent Fermi interaction terms have to be fitted simultaneously with three yet unknown band centers. A stronger confinement of the initial parameters, by fixing the three interaction terms derived from the $K = 2$ subband, did not yield satisfactory results either, which is why, similar to the approach used by Amano,[5] second-order perturbation theory might be used for the $K = 1$ subband instead of the direct deperturbation fit within PGOPHER. However, the interacting states might be very close in energy such that higher order perturbations would be needed. Because of these open questions a simplistic approach has been taken motivated by some basic considerations instead.

According to the treatment of a pairwise Fermi resonance the resulting energy shifts leave the average value of the energy of two participating levels, say E_A and E_B, constant, i.e., $(E'_A + E'_B)/2 = (E_A + E_B)/2$. Here E'_A and E'_B are the energies of the perturbed system from eq 1. In fact, this holds for the band as a whole and the subbands as well, as long as the Fermi term is considered independent of J, i.e., $W_{A,B}(J, K) = W_{A,B}(K)$ as found for the $K = 0$ and 2 subbands so far. Due to this sum rule also the sum of the energies of all contributing levels remains the same, and this should hold also for a system of many interacting levels.

From a mathematical point of view the deperturbation of the interacting Fermi system corresponds to a diagonalization of the energy matrix. The trace of the perturbed matrix is the sum of the energies E_i of the system without consideration of the Fermi interaction, $\sum_i E_i$, where the sum includes all (finally) interacting vibrations. The diagonalization is associated with a change of basis sets, i.e., by similarity transformations, which leaves the trace of the matrix unchanged. For the energies of the interacting Fermi system this means, $\sum_i E'_i = \sum_i E_i$, where E'_i are now the energies of the perturbed system. Therefore, the sum rule for two interacting Fermi levels also holds for many interacting levels.

For $K = 1$ it applies for the six participating vibrations analyzed in Table 3. In fact, it holds for each rotational level J which means that the sum of all rotational constants of the perturbed and unperturbed levels remains constant. Since all participating bands arise from the same vibrational ground state, also the sum of the rotation-vibration interaction terms remains unchanged in the perturbed ($\alpha_i'^B$) and unperturbed (α_i^B) system, i.e.

$$\sum_i \alpha_i'^B = \sum_i \alpha_i^B \tag{2}$$

Assuming the unperturbed rotation-vibration coupling constants, α_i^B, of Bands I, III, and IV to be adequately determined by our deperturbation of the $K = 0$ and $K = 2$ subbands, the sum rule of eq 2 leads to an average rotation-vibration interaction constant of the three yet unknown combination bands of $\bar{\alpha}_{II,V,VI}^B = -64.1(5)$ MHz, when the $\alpha_i'^B$ for the six participating bands are taken from Table 3. Unfortunately, the third three-quanta combination band lying close to the ν_2 fundamental, the $\nu_4 + \nu_8 + \nu_9$ combination, would only have one additional A_1-symmetry component thus only giving rise to one of the three additional interacting combination bands. Furthermore, its calculated rotation-vibration interaction constant is $\alpha_{\nu_4+\nu_8+\nu_9}^B = 59$ MHz, which is significantly different from the derived average rotation-vibration interaction constant. As no other combination band with up to three vibrational quanta is found to be in reasonable proximity to the ν_2 fundamental, the likelihood of the $\nu_4 + \nu_8 + \nu_9$ combination band affecting the Fermi-resonance system appears to be relatively low. It seems more likely that combinations of four or more vibrational quanta have to be considered, as the combination of four degenerate (E-symmetry) vibrational fundamentals would result in a combination band having three A_1-, three A_2-, and five E-symmetry components. Indeed, combining the anharmonic vibrational frequencies listed in Table 1, it turns out that the $\nu_7 + 2\nu_9 + \nu_{10}$ combination band would be approximately 44 cm^{-1} above the ν_2 fundamental as displayed in the left panel of Figure 2. Based on our quantum chemical calculations, the rotation-vibration interaction con-

https://doi.org/10.1021/acs.jpca.5c06360
J. Phys. Chem. A 2026, 130, 88−95

stant of this combination band is estimated to be $\alpha^{B}_{\nu_7+2\nu_9+\nu_{10}}$ = −73.3 MHz, which is reasonably close to the average rotation-vibration interaction constant derived above. However, even using these findings in a direct deperturbation fit using PGOPHER[28] did not lead to a converging fit. Therefore, these three additional bands could only be assigned tentatively to the A_1-symmetry components of the $\nu_7 + 2\nu_9 + \nu_{10}$ combination band. This is why these three energy levels (II, V, and VI) are plotted together with the three deperturbed levels (I, III, and IV) in the right panel of Figure 2 for the $K = 1$ Fermi system. Altogether, Figure 2 shows the richness of the ν_2 Fermi resonance system whose energy levels have been determined very accurately by the current analysis of the high-resolution spectrum of the ν_2 vibrational Fermi system.

CONCLUSIONS

After the detection of the ν_1 band of CH_3CNH^+ more than 30 years ago,[5] the first spectroscopic observation of this molecule, this work reports on the second vibrational band recorded at high resolution, the ν_2 symmetric CH_3 stretching vibration using the LOS technique. In the former work,[5] the ν_2 symmetric and the ν_6 antisymmetric CH_3 stretching vibrations were avoided due to spectral interference of lines of the neutral CH_3CN precursor. However, the mass selectivity and cryogenic cooling of the experimental technique used here enabled the rapid identification of the involved transitions of the symmetric CH_3 stretching mode. Several interfering combination bands were detected close to the ν_2 fundamental, which, based on direct deperturbation fits, could be assigned as the $\nu_5 + 2\nu_8$ as well as the $\nu_5 + \nu_7 + \nu_9$ combination bands. A possible four-quanta combination band, $\nu_7 + 2\nu_9 + \nu_{10}$, is tentatively assigned to affect the $K = 1$ subband based on fundamental considerations of a Fermi resonance system. All findings are in good agreement with previous studies of other methyl compounds, such as methyl acetylene[31] or the ν_1 band of protonated methyl cyanide itself.[5] While the Fermi resonances lead to a rather complex spectrum, the interplay of the high-quality infrared spectra and the high-level calculations presented here with the highly accurate molecular parameters of the ground state from previous work[6,7] led to very reliable molecular parameters for three of the interacting bands and to a rather confident assignment of all bands. Therefore, the procedure of successful deperturbation described in this work will be a guideline for the ro-vibrational analysis of other molecules which exhibit Fermi resonances of close-lying vibrational bands.

The only molecular parameter missing for protonated methyl cyanide from experiment is the rotational constant A, because all hitherto measured vibrational bands as well as the pure rotational spectrum follow predominantly $\Delta K = 0$ selection rules. In future studies A may be derived from high-resolution LOS measurements of the ν_6 antisymmetric CH_3 stretching vibration, a perpendicular band ($\Delta K = \pm 1$), predicted and measured[8] at about 3002 cm^{-1}, see also Table 1.

ASSOCIATED CONTENT

Supporting Information

The Supporting Information is available free of charge at https://pubs.acs.org/doi/10.1021/acs.jpca.5c06360.

ASCII data of the spectrum shown in Figure 1, as well as its assigned line list, and energy term diagram shown in Figure 2 is presented to display the experimental results without any model assumptions (PDF)

AUTHOR INFORMATION

Corresponding Author

Stephan Schlemmer − *I. Physikalisches Institut, Universität zu Köln, D-50937 Köln, Germany;* orcid.org/0000-0002-1421-7281; Email: schlemmer@ph1.uni-koeln.de

Authors

Thomas Salomon − *I. Physikalisches Institut, Universität zu Köln, D-50937 Köln, Germany;* orcid.org/0000-0003-4068-7444

Weslley G. D. P. Silva − *I. Physikalisches Institut, Universität zu Köln, D-50937 Köln, Germany;* orcid.org/0000-0001-8775-8815

Sven Thorwirth − *I. Physikalisches Institut, Universität zu Köln, D-50937 Köln, Germany;* orcid.org/0000-0001-8200-6710

Oskar Asvany − *I. Physikalisches Institut, Universität zu Köln, D-50937 Köln, Germany;* orcid.org/0000-0003-2995-0803

Complete contact information is available at: https://pubs.acs.org/10.1021/acs.jpca.5c06360

Notes

The authors declare no competing financial interest.

ACKNOWLEDGMENTS

This work has been supported by an ERC Advanced Grant (MissIons: 101020583), and by the Deutsche Forschungsgemeinschaft (DFG) via the Collaborative Research Centre SFB 1601 (project ID: 500700252, subproject C4 and B8) and via SCHL 341/15-1 ("Cologne Center for Terahertz Spectroscopy"). The Toptica cw-OPO has also been financed by DFG (INST 216/1184-1, project number 504504934). W.G.D.P.S. thanks the Alexander von Humboldt Foundation for support through a postdoctoral fellowship. We thank Joshua Karner for support in the laboratory measurements.

REFERENCES

(1) Solomon, P. M.; Jefferts, K. B.; Penzias, A. A.; Wilson, R. W. Detection of Millimeter Emission Lines from Interstellar Methyl Cyanide. *Astrophys. J. Lett.* **1971**, *168*, No. L107.

(2) Giani, L.; Ceccarelli, C.; Mancini, L.; Bianchi, E.; Pirani, F.; Rosi, M.; Balucani, N. Revised gas-phase formation network of methyl cyanide: the origin of methyl cyanide and methanol abundance correlation in hot corinos. *Mon. Not. R. Astron. Soc.* **2023**, *526*, 4535−4556.

(3) Knight, J. S.; Freeman, C. G.; McEwan, M. J. Isomers of $C_2H_4N^+$ and the proton affinities of acetonitrile and methyl isocyanide. *J. Am. Chem. Soc.* **1986**, *108*, 1404−1408.

(4) Turner, B. E.; Amano, T.; Feldman, P. A. Searches for the Protonated Interstellar Species HC_3NH^+, CH_3CNH^+, and $HOCS^+$: Implications for Ion−Molecule Chemistry. *Astrophys. J.* **1990**, *349*, 376−387.

(5) Amano, T. Difference frequency laser spectroscopy of the ν_1 fundamental band of CH_3CNH^+. *J. Mol. Spectrosc.* **1992**, *153*, 654−665.

(6) Amano, T.; Hashimoto, K.; Hirao, T. Submillimeter-wave spectroscopy of $HCNH^+$ and CH_3CNH^+. *J. Mol. Struct.* **2006**, *795*, 190−193.

(7) Gottlieb, C. A.; Apponi, A. J.; McCarthy, M. C.; Thaddeus, P.; Linnartz, H. The rotational spectra of the HCCCNH$^+$, NCCNH$^+$, and CH_3CNH^+ ions. *J. Chem. Phys.* **2000**, *113*, 1910−1915.
(8) Marimuthu, A. N.; in't Veld, F. H.; Thorwirth, S.; Redlich, B.; Brünken, S. Infrared predissociation spectroscopy of protonated methyl cyanide, CH_3CNH^+. *J. Mol. Spectrosc.* **2021**, *379*, No. 111477.
(9) Schmid, P. C.; Asvany, O.; Salomon, T.; Thorwirth, S.; Schlemmer, S. Leak-out Spectroscopy, a universal method of action spectroscopy in cold ion traps. *J. Phys. Chem. A* **2022**, *126*, 8111−8117.
(10) Asvany, O.; Brünken, S.; Kluge, L.; Schlemmer, S. COLTRAP: a 22-pole ion trapping machine for spectroscopy at 4 K. *Appl. Phys. B: Laser Opt.* **2014**, *114*, 203−211.
(11) Asvany, O.; Bielau, F.; Moratschke, D.; Krause, J.; Schlemmer, S. New design of a cryogenic linear RF multipole trap. *Rev. Sci. Instrum.* **2010**, *81*, No. 076102.
(12) Asvany, O.; Thorwirth, S.; Schmid, P. C.; Salomon, T.; Schlemmer, S. High-resolution ro-vibrational and rotational spectroscopy of HC_3O^+. *Phys. Chem. Chem. Phys.* **2023**, *25*, 19740−19749.
(13) Bast, M.; Böing, J.; Salomon, T.; Thorwirth, S.; Asvany, O.; Schäfer, M.; Schlemmer, S. Ro-vibrational spectra of CC stretching modes of C_3H^+ and HC_3O^+. *J. Mol. Spectrosc.* **2023**, *398*, No. 111840.
(14) Schlemmer, S.; Plaar, E.; Gupta, D.; Silva, W. G. D. P.; Salomon, T.; Asvany, O. High-resolution spectroscopy of the ν_3 antisymmetric C−H stretch of $C_2H_2^+$ using leak-out action spectroscopy. *Mol. Phys.* **2024**, *122*, No. e2241567.
(15) Silva, W. G. D. P.; Cernicharo, J.; Schlemmer, S.; et al. Discovery of H_2CCCH^+ in TMC-1. *Astron. Astrophys.* **2023**, *676*, No. L1.
(16) Silva, W. G. D. P.; Gupta, D.; Plaar, E.; Doménech, J. L.; Schlemmer, S.; Asvany, O. High resolution rovibrational and rotational spectroscopy of H_2CCCH^+. *Mol. Phys.* **2024**, *122*, No. e2296613.
(17) Gupta, D.; Silva, W. G. D. P.; Doménech, J. L.; Plaar, E.; Thorwirth, S.; Schlemmer, S.; Asvany, O. High-resolution rovibrational and rotational spectroscopy of the singly deuterated cyclopropenyl cation, c-$C_3H_2D^+$. *Faraday Discuss.* **2023**, *245*, 298−308.
(18) Steenbakkers, K.; van Boxtel, T.; Groenenboom, G. C.; Asvany, O.; Redlich, B.; Schlemmer, S.; Brünken, S. Leak-out spectroscopy as alternative method to rare-gas tagging for the Renner−Teller perturbed HCCH$^+$ and DCCD$^+$ ions. *Phys. Chem. Chem. Phys.* **2024**, *26*, 2692−2703.
(19) Silva, W. G. D. P.; Bonah, L.; Schmid, P. C.; Schlemmer, S.; Asvany, O. Hyperfine-resolved rotational spectroscopy of HCNH$^+$. *J. Chem. Phys.* **2024**, *160*, No. 071101.
(20) Salomon, T.; Baddeliyanage, C.; Schladt, C.; Simkó, I.; Császár, A. G.; Silva, W. G. D. P.; Schlemmer, S.; Asvany, O. High-resolution leak-out spectroscopy of HHe_2^+. *Phys. Chem. Chem. Phys.* **2025**, *27*, 4826−4828.
(21) Gupta, D.; Schmid, P. C.; Salomon, T.; Asvany, O.; Schlemmer, S. Rotationally Resolved Spectrum of the Degenerate Antisymmetric C−H Stretching Band of c-$C_3H_3^+$. *ACS Earth Space Chem.* **2025**, *9*, 952−958.
(22) McCaslin, L.; Stanton, J. F. Calculation of fundamental frequencies for small polyatomic molecules: a comparison between correlation consistent and atomic natural orbital basis sets. *Mol. Phys.* **2013**, *111*, 1492−1496.
(23) Matthews, D. A.; Cheng, L.; Harding, M. E.; Lipparini, F.; Stopkowicz, S.; Jagau, T.-C.; Szalay, P. G.; Gauss, J.; Stanton, J. F. Coupled-cluster techniques for computational chemistry: The CFOUR program package. *J. Chem. Phys.* **2020**, *152*, No. 214108.
(24) Harding, M. E.; Metzroth, T.; Gauss, J.; Auer, A. A. Parallel calculation of CCSD and CCSD(T) analytic first and second derivatives. *J. Chem. Theory Comput.* **2008**, *4*, 64−74.
(25) Puzzarini, C.; Stanton, J. F.; Gauss, J. Quantum-chemical calculation of spectroscopic parameters for rotational spectroscopy. *Int. Rev. Phys. Chem.* **2010**, *29*, 273−367.
(26) Cazzoli, G.; Puzzarini, C. Lamb-dip spectrum of methylacetylene and methyldiacetylene: precise rotational transition frequencies and parameters of the main isotopic species. *Astron. Astrophys.* **2008**, *487*, 1197−1202.
(27) Müller, H. S.; Belloche, A.; Lewen, F.; Drouin, B. J.; Sung, K.; Garrod, R. T.; Menten, K. M. Toward a global model of the interactions in low-lying states of methyl cyanide: Rotational and rovibrational spectroscopy of the ν_4 = 1 state and and tentative interstellar detection of the ν_4 = ν_8 = 1 state in Sgr B2(N). *J. Mol. Spectrosc.* **2021**, *378*, No. 111449.
(28) Western, C. M. PGOPHER: A program for simulating rotational, vibrational and electronic spectra. *J. Quant. Spectrosc. Radiat. Transfer* **2017**, *186*, 221−242.
(29) Brackertz, S.; Schlemmer, S.; Asvany, O. Searching for new symmetry species of CH_5^+ − From lines to states without a model. *J. Mol. Spectrosc.* **2017**, *342*, 73−82.
(30) Cerqueira, H. B. A.; Santos, J. C.; Fantuzzi, F.; de A Ribeiro, F.; Rocco, M. L. M.; Oliveira, R. R.; Rocha, A. B. Structure, Stability, and Spectroscopic Properties of Small Acetonitrile Cation Clusters. *J. Phys. Chem. A* **2020**, *124*, 6845−6855.
(31) Boyd, D. R. J.; Thompson, H. The infra-red spectrum of methyl acetylene. *Trans. Faraday Soc.* **1952**, *48*, 493−501.

https://doi.org/10.1021/acs.jpca.5c06360
J. Phys. Chem. A 2026, 130, 88−95